Ni–Mo and Ni–W sulfide catalysts prepared by decomposition of binary thiometallates

F. Pedraza * and S. Fuentes **

Instituto Mexicano del Petróleo, Programa de Simulacióm Molecular, Edif. 23, Ofic. 222, Eje Central L. Cárdenas No. 152, Apdo Postal 14-805, CP 07730, México DF, Mexico
E-mail: lpedraza@www.imp.mx

Received 12 September 1999; accepted 14 January 2000

Ni–Mo and Ni–W sulfide catalysts with atomic ratio $R = 0.5$ (Ni/(Ni + M), with M = Mo or W) prepared by decomposition of Ni-impregnated thiometallates were evaluated in the reaction of thiophene hydrodesulfurization. Catalysts derived from impregnated thiometallates (DTI samples) presented improved catalytic activity and higher synergistic effect than catalysts prepared by co-precipitation (HSP samples) despite the fact that co-precipitated catalysts showed larger surface area. Structure characterization by high-resolution electron microscopy (HREM) and X-ray diffraction (XRD) revealed different crystalline phases in DTI and HSP catalysts. A mixture of phases (MS_2, $NiS_{1.03}$ and MO_2) was observed in catalysts obtained by co-precipitation. Only the poorly crystalline MS_2 phase was observed in DTI catalysts suggesting that the Ni promoter is very well dispersed on the chalcogenide structure.

Keywords: thiometallates decomposition, hydrodesulfurization, Ni–Mo sulfide, Ni–W sulfide, synergistic effect

1. Introduction

The application of bis-thiometallate complexes as precursors for the preparation of hydrotreating catalysts was reported some years ago [1,2]. Stiefel et al. [1] reported binary sulfide catalysts (Co–Mo, Ni–Mo, Co–W and Ni–W) active for the hydrodesulfurization of dibenzothiophene, obtained by thermal decomposition of bis-tetrathiometallate precursors in the temperature range 300–400 °C, in presence of sulfur and hydrogen and most preferentially in presence of a sulfur-bearing hydrocarbon.

Eltzner et al. [2] reported that decomposed bis-thiometallate complexes show an activity two to three times higher than the corresponding co-precipitated catalysts in the hydrogenation of biphenyl. They suggested that mixed M–S–M′–S–M units already shown in the bis-thiometallate precursor remain in the catalyst after decomposition of the precursor.

Other kinds of binary complexes involving Ni and Mo or W are the chelate type complexes such as the $Ni(en)_3MS_4$. The use of chelating agents such as the nitriloacetic acid (NTA) and ethylene-diamine-tetra-acetic acid (EDTA) during the impregnation of Co–Mo/Al_2O_3, Ni–Mo/Al_2O_3 and Ni–W/Al_2O_3 catalysts resulted in higher HDS and hydrogenation activity than those of the catalysts prepared without the chelating agents [3–6].

A method involving the preparation of catalysts through the decomposition of thiosalts impregnated with the promoter (DTI) was reported by Fuentes et al. [7]. They compared the catalytic properties of Co–Mo and Ni–Mo catalysts prepared by two methods, the homogeneous sulfide precipitation (HSP) and the decomposition of an impregnated thiosalt (DTI). The DTI catalysts presented improved catalytic activity compared to HSP catalysts for the hydrogenation of biphenyl, the hydrogenation of cyclohexene as well as the HDS of thiophene. The improved activity was attributed to the formation of higher concentration of active Ni–Mo and Co–Mo sites in the DTI method [8].

In the present work a further study about the structural and catalytic properties of Ni–Mo and Ni–W catalysts obtained by DTI and HSP is performed. The effect of precursors on the catalytic and structural properties of catalysts is analyzed. The synergistic effect observed in the thiophene hydrodesulfurization reaction is discussed in terms of the dispersion of the nickel promoter and the electronic interaction with MoS_2 and WS_2.

2. Experimental

The NiMo and NiW binary precursors used in the DTI series were obtained according to the method reported by Fuentes et al. [7]. In that method, the thiosalt (ammonium thiomolybdate or ammonium thiotungstate) is reacted with the promoter (nickel nitrate) in acetone forming a brown precipitate. After evaporation of the solvent a solid precursor containing both metals Ni and Mo or W was separated. Binary co-precipitated samples (HSP precursors) were prepared following the procedure reported by Candia et al. [9]. Both types of precursor were treated under a reducing–sulfiding atmosphere of 15 vol% H_2S in H_2 during 4 h at 673 K. After cooling to room temperature the

* To whom correspondence should be addressed.
** On leave from Centro de Ciencias de la Materia Condensada-UNAM, Ensenada.

catalysts were purged with nitrogen and stored in sealed bottles under argon.

Specific BET surface areas were measured with a Micromeritics Gemini 2060 surface area analyzer, using nitrogen adsorption at 77 K. Samples were degassed under flowing argon at 473 K for 2 h before nitrogen adsorption.

The catalytic activities were determined during the HDS of thiophene. This reaction test was carried out in the vapor phase using a dynamic atmospheric pressure microreactor. The specific rate (R_s) is calculated using the following reaction:

$$R_s = F_a C/m \text{ (mol/s g)},$$

where F_a is the thiophene molar flow (mol/s), C is conversion, and m is catalyst weight (g).

XRD experiments of the resulting catalysts were performed in a Philips X'PERT.MPD analytical diffractometer, equipped with a curved graphite monochromator, using Cu K_α radiation ($\lambda = 0.154178$ nm).

HREM micrographs were obtained in a Jeol 4000 EX transmission electron microscope with a point to point resolution of 0.17 nm. Catalyst samples were ground with a mullite mortar and pestle and were ultrasonically dispersed in heptane. A drop of the suspension was air-dried in a carbon-coated electron microscope grid for examination in the microscope.

Elemental analysis was performed by means of electron dispersive spectroscopy (EDS) in a Jeol 5300 electron microscope equipped with a Quantum window.

3. Results

3.1. Surface area

The surface areas of catalysts were determined before and after the catalytic test reaction; results are shown in table 1. The MoS_2 and WS_2 catalysts showed surface area values (40–50 m^2/g) that are typical for samples obtained by decomposition of thiosalts [10–12]. The surface area of MoS_2 after the catalytic test was 10 m^2/g indicating that a drastic diminution of surface area occurred during the catalytic reaction. A similar effect was observed for the NiS catalyst that decreased from 4 to 1 m^2/g. In contrast to monometallic sulfides, the surface areas of binary sulfide catalysts remained almost the same after the catalytic test. The NiW catalysts presented higher surface areas than the WS_2 catalyst. Otherwise the NiMo catalysts showed lower surface areas than the MoS_2 catalyst. In general, HSP catalysts showed higher surface area values than DTI ones.

3.2. Elemental analysis

The elemental analysis of the NiW catalysts is reported in table 2. The DTI catalyst shows slightly lower amount of W and higher amount of S than the HSP catalyst. The measured ratio R (Ni/(Ni + W)) for both types of catalyst DTI (0.52) and HSP (0.50) was close to the nominal ratio (0.5). The compositions of NiMo catalysts were not calculated because the peaks of S and Mo appear superimposed making difficult a quantitative estimation. However, the same tendencies in composition of NiW catalysts were observed in NiMo catalysts.

Table 1
Surface areas of catalysts before and after the catalytic test.

Sample	Initial area S_i (m^2/g)	Final area S_f (m^2/g)
NiS	4	1
Ni–W (HSP)	62	–
Ni–W (DTI)	52	48
WS_2	41	–
Ni–Mo (HSP)	35	30
Ni–Mo (DTI)	21	17
MoS_2	51	11

Table 2
Elemental analysis by EDS.

Catalyst	Weight (%)			Atomic (%)			R
	Ni	W	S	Ni	W	S	[Ni/(Ni + W)]
NiW (DTI)	20.5	57.9	21.6	26.1	23.5	50.3	0.52
NiW (HSP)	20.2	63.2	16.6	28.6	28.5	43.0	0.5

3.3. X-ray diffraction

Figure 1 shows the diffraction pattern for all catalysts. Both, MoS_2 and WS_2 catalysts had diffraction patterns corresponding with the 2H-hcp structures reported in the ICDPDF files. In the case of mixed catalysts the prevalent features were those of the MoS_2 or WS_2 structures with additional phases in some cases.

In HSP Ni–Mo catalysts, besides the MoS_2-2H structure, the MoO_2, $NiS_{1.03}$ and NiS (synthetic millerite) phases were observed. In DTI Ni–Mo catalysts the MoS_2-2H phase was mainly observed, although minor traces of $NiS_{1.03}$ were detected.

The Ni–W catalysts presented similar XRD patterns as those found for Ni–Mo catalysts. In the HSP Ni–W catalysts besides the WS_2-2H structure, other phases as $NiS_{1.03}$ and WO_2 were found. In the DTI Ni–W catalysts the WS_2-2H phase was mainly observed with minor traces of $NiS_{1.03}$.

3.4. High-resolution electron microscopy

High-resolution micrographs of MoS_2 and WS_2 catalysts were similar to those reported in previous works [13] and, therefore, they are not shown. The catalyst structure coincided with the poor crystalline structure reported by Liang et al. [14], where folded, rotated and shifted planes, which are characteristic of a very disordered structure, were found.

The electron micrographs of NiMo and NiW HSP catalysts shown in figure 2 reveal two cases:

(1) NiS particles surrounded by MoS_2 (figure 2(a)) and WS_2 (figure 2(b)) layers;

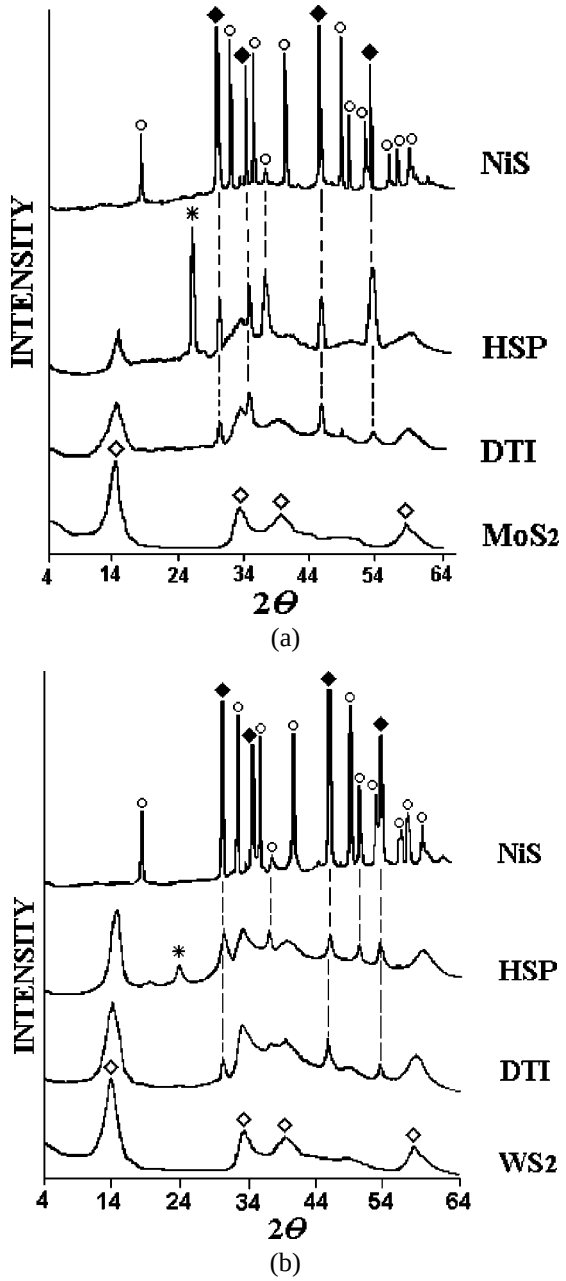

Figure 1. (a) Diffraction pattern for Ni–Mo: (◊) MoS_2-2H, (∗) MoO_2, (♦) $NiS_{1.03}$ and (○) NiS millerite. (b) Diffraction pattern for Ni–W: (◊) WS_2-2H, (∗) WO_2, (♦) $NiS_{1.03}$ and (○) NiS millerite.

(2) NiS particles deposited on top of MoS_2 particles (figure 2(c)).

The micrographs of DTI sulfides in figure 3 show MoS_2 (figure 3(a)) and WS_2 (figure 3(b)) particles presenting the (100) lattice resolution. In these catalysts nickel sulfide particles were not observed.

3.5. Catalytic activity

The specific and intrinsic rates for the HDS of thiophene measured at 573 K are reported in table 3. The DTI Ni–Mo and Ni–W catalysts showed higher activities than their respective HSP catalysts (the relative ratio of intrinsic rates DTI/HSP was 2 for Ni–W and 2.8 for Ni–Mo). A greater catalytic activity was observed in DTI catalysts despite that their surface areas were significantly lower than those of HSP catalysts. The synergistic effect was also larger for the DTI catalysts than for the HSP ones. It was also observed that the Ni–Mo catalysts were more active for the thiophene HDS reaction than their respective Ni–W catalysts.

4. Discussion

4.1. Decomposition of the DTI precursors

The reaction occurring in the DTI method between the promoter and the ammonium thiosalt to form the binary thiometallate precursor may be written as

$$2(NH_4)_2MS_4 + M'(NO_3)_2 \rightarrow (NH_4)_2\{M'(MS_4)_2\} + 2NH_4NO_3 \quad (1)$$

where M is Mo or W, and M′ is Ni or Co. In this step, the promoter cation is bonded to the thioanion containing the Mo or W atom.

The decomposition of the binary ammonium thiometallate obtained through reaction (1), in presence of hydrogen gives the binary sulfides according to the reactions

$$M'(MS_4)_2 + H_2 \rightarrow M'(MS_3)_2 + H_2S \quad (2)$$

$$M'(MS_3)_2 + H_2 \rightarrow M'(MS_2)_2 + H_2S \quad (3)$$

By these means, the chemical interaction produced during the formation of the binary thiometallates is maintained in the NiMo and NiW catalysts and the electronic properties of the binary thiometallate precursors are preserved in the NiMo and NiW catalysts. It is suggested that this process occur in a similar way to the case of the tri-ethylamine bis-thiometallate of Co and Mo [15,16]. Also in the case of Ni and Mo complexes, it has been shown [2] that the electronic spectra of Ni–Mo sulfide catalysts derived from alkyl-thiometallates coincide with that of the precursor. Hence, the electronic interaction occurring in the binary unit $M'(MS_4)_2$ between the promoter in the precursor and which is kept on the catalyst enhances the electron availability of the valence band (see above).

The preserving of the chemical interaction among Ni and Mo or W atoms after the decomposition process also implies that a good dispersion of the promoter in MoS_2 or WS_2 is obtained, forming a large number of NiMo or NiW sites. These sites located on the edge of MoS_2 or WS_2 crystallites are proposed to act as the active sites for hydrotreating processes.

In summary, the reactions of synthesis of thiometallates and their decomposition can be both carefully controlled leading to a better dispersion of the promoter in the catalyst.

It has to be noticed that the metal ratio R obtained through these reactions is different from the ratio observed experimentally by EDS ($R = 0.33$ instead of 0.5) indicating that some excess of nickel sulfide is present in the

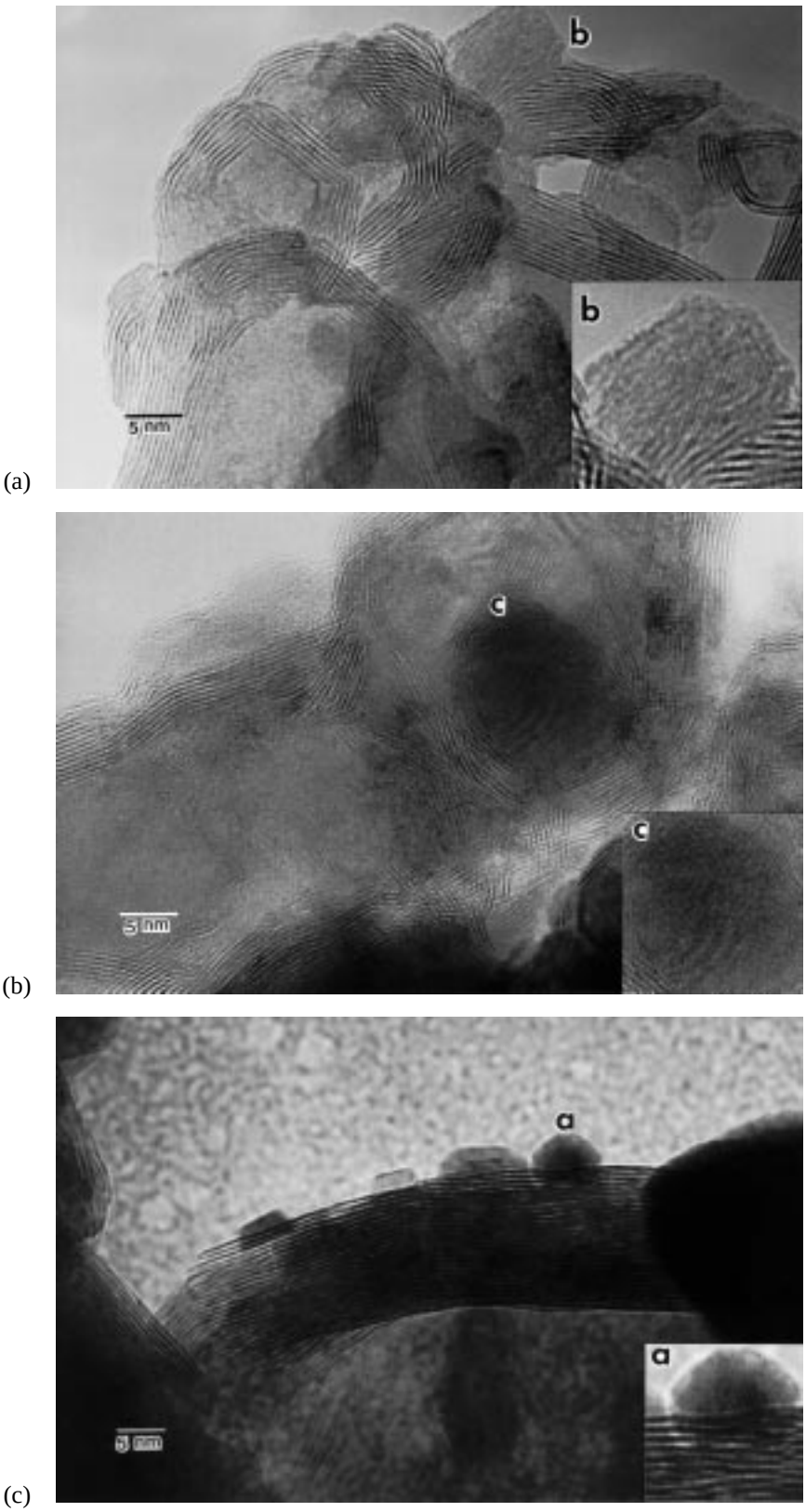

Figure 2. HRTEM micrographs of binary HSP catalysts: NiS particles surrounded by MoS_2 (a) and WS_2 (b) layers, NiS particles deposited on top of MoS_2 particles (c).

ITD catalysts. Nevertheless, no evidence of nickel sulfide crystalline phases was observed by XRD and HRTEM in DTI catalysts, suggesting that such excess of nickel sulfide is very well dispersed over the catalyst too. Further studies are needed to put in evidence the nature of this nickel sulfide in excess and that could be in the form of an amor-

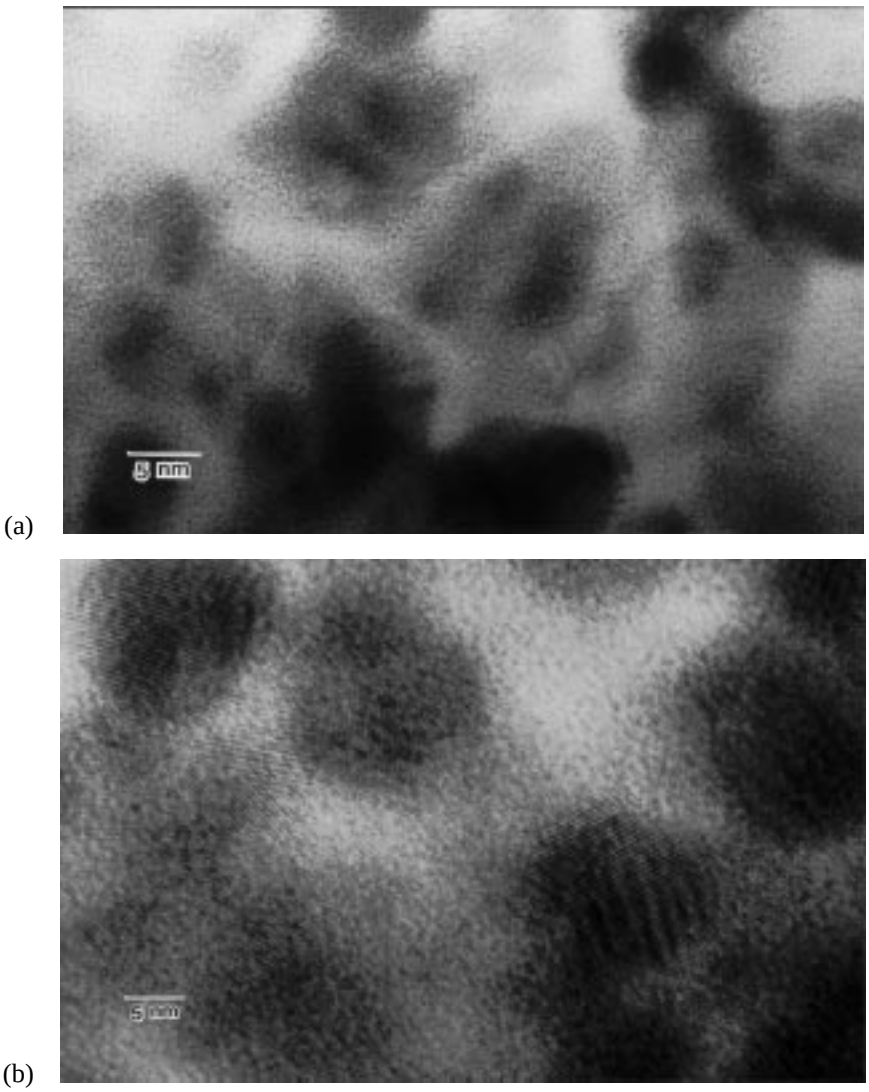

Figure 3. HRTEM micrographs of binary DTI sulfides: (a) Ni–Mo and (b) Ni–W.

Table 3
Catalytic activity of Ni–Mo and Ni–W.

Catalyst	R [Ni/(Ni + Mo (W))] Exp. value	Specific rate (10^6 mol/g s)	Intrinsic rate (10^{-8} mol/m^2 s)
NiS	1.00	0.05	1.25
Ni–W (HSP)	0.50	1.57	2.53
Ni–W (DTI)	0.52	2.62	5.04
WS_2	0.00	0.24	0.58
Ni–Mo (HSP)	0.50	1.75	5.00
Ni–Mo (DTI)	0.49	2.93	14.00
MoS_2	0.00	0.26	0.51

phous structure or very small crystallites or epitaxial layers of nickel sulfide.

4.2. Surface area

The HSP catalysts show higher surface areas than DTI catalysts. This is mainly due to the large size of the thiometallate crystals used as precursors (several microns) compared with the small size of particles obtained by precipitation (few nanometers). During thiometallate decomposition NH_3 and H_2S gases are evolved generating a porous structure in the particles of MoS_2. It has been shown that surface area of DTI catalysts is only due to the internal porosity of the particles and is not affected by changes in the size of the ATM crystal [17]. In the HSP method, depending on the pH of the metal salt solution, different species (e.g., heteropoly-anions, thio-anions and metal sulfur clusters), are generated besides of the disulfides. In the reducing–sulfiding treatment of precipitated precursors some chemical changes occur, the oxide and hydrated species are sulfided and small particles of meta-stable sulfides are transformed to stable phases. These processes affect the porous structure decreasing the initial surface area. It has been reported that surface area of nickel sulfide precursors obtained by precipitation decreases from 20 to 4 m^2/g when the precursor is treated under 15% H_2S in hydrogen for 4 h at 673 K [18]. Nevertheless, due to the very large difference of particle size between the thiometallate crystal (several microns) and the precipitated particles (few nanometers), the external surface

of the precipitated catalyst remains larger than the internal surface of the thiometallate derived catalysts.

The decrease of surface area observed in MoS_2 catalysts due to the catalytic test was attributed previously to sintering of MoS_2 crystallites [17] that grow laterally through the edges, causing at the same time a decrease of the activity and the surface area. In the same way, the stability of surface area of binary sulfides during the catalytic test can be attributed to the promoter atoms attached to the edges, that stabilize MoS_2 particles and increase the activity through formation of Ni–M–S active sites.

4.3. Structural characterization

The structural characterization by HREM and XRD revealed that HSP catalysts presented a mixture of sulfide and oxide phases while DTI catalysts presented only a uniform phase. As mentioned below, the precipitation method involves several reactions that cause that the final catalyst is not uniform, presenting several phases. The phases observed in HSP catalysts by X-ray diffraction and transmission electron microscopy coincided with those reported in the phase diagram of Pratt and Sanders for similar catalysts [19]. The HSP method led to NiW catalysts with composition $NiWS_{1.5}$.

The decomposition of thiosalts (ammonium thiomolybdate or ammonium thiotungstate) is a well-known process rendering MS_3 as an intermediate and MS_2 as the final product. Following a similar scheme, the decomposition of bis-thiometallate complexes of the type $(Et_4N)_3[Co(MoS_4)_2]$ reported by Eltzner [2] forms a binary sulfide of composition $CoMo_2S_6$ in N_2 atmosphere, meanwhile in 15% H_2S in H_2 shows slightly higher weight losses leading to solids with composition $M'M_2S_{5-6}$. In our case, the decomposition of the binary thiometallates in 15% H_2S in hydrogen led to catalysts with composition $Ni_{1.1}WS_{2.14}$.

The X-ray diffraction pattern reported for binary sulfides obtained by ITD is similar to the diffraction pattern of MoS_2 or WS_2, which in turn are characteristic of the "poorly crystalline" sulfide.

The structures of HSP Ni–Mo and Ni–W catalysts observed by TEM showed that MoS_2 structures were surrounding NiS particles or mounted on top of them. These structures are similar to those reported by Pratt and Sanders for MoS_2 [20], Garreau et al. for Ni–Mo [21], and Blanchard et al. for Ni–W [22]. The driving force for these phenomena is the chemical reactivity of edge planes of MoS_2 that preferentially react with NiS or MoO_2 structures inducing epitaxial growth of MoS_2 on top of them.

4.4. Catalytic activity

Both Ni–W and Ni–Mo DTI catalysts show higher intrinsic rates than their respective HSP catalysts. For Ni–Mo catalysts the DTI/HSP ratio of rates is 2.8 while for Ni–W catalysts it is 2.1. It suggests that a higher amount of active sites per surface area unit were obtained with the DTI method. A possible explanation can be related with the increased amount of active sites in MoS_2 obtained from ATM as suggested by Iwata [23] and the increased dispersion of the promoter on these sites. The fact that only the structure of the active phase is observed by TEM in DTI catalysts while crystalline phases containing the promoter are detected in HSP ones, clearly indicates that an increased dispersion of the promoter was achieved in the former despite their lower surface area.

The large promoter effect of Ni in MoS_2 and WS_2 catalysts in DTI is related to the electronic interactions occurring in the precursor and that remain between the promoter and the active phase in the catalyst. The enhanced dispersion of nickel on MoS_2 and WS_2 in the DTI catalysts compensates their lower surface area when compared to the HSP catalysts overcoming on their catalytic activity.

The higher catalytic activity of Ni–Mo over Ni–W catalysts is explained because Ni–Mo catalysts are superior to Ni–W catalysts for feedstock containing high amount of sulfur. An alternative explanation could be that Ni–Mo catalysts are more resistant to poisoning by H_2S than Ni–W catalysts [24,25].

4.5. Electronic properties

The electronic structures of Ni–Mo and Ni–W complexes have been characterized by XPS and EXAFS [18, 19,26,27].

In $(MoS_4)^{2-}$ and $(WS_4)^{2-}$ anions, Mo and W atoms are tetrahedrally coordinated to S atoms with T_d symmetry. The MoS_4^{2-} unit can behave as double bridging ligands symmetrically coordinated to other MoS_4^{2-} units or to M′ cations. They can also form chains of tetrahedral units connected via edges [26].

The XPS spectra of binary sulfide catalysts NiMoS and NiWS reflect a similar situation as the spectra of the bis-thiometallate complexes. They show typical bands representative of electronic delocalization $Ni \rightarrow (MS_4)^{2-}$ [18].

The X-ray absorption spectra (EXAFS) of bis-thiometallates performed by Wittneben et al. [19], for the sulfur-edge spectra (2460 and 2505 eV) revealed absorption peaks in agreement with SCF-X_α calculations. The characteristic spectra of MS_4^{2-} (M = Mo or W) and $[Ni(MS_4)_2]^{2-}$ in the pre-edge region revealed that tungsten anion shows three absorption peaks corresponding to electron transitions from the 1s level to the e, t_2 and a_1 levels, meanwhile, molybdenum anions show only two absorption peaks, one for $1s \rightarrow t_2$ and a_1 transitions, which are very close each other and then remain unresolved, and other for the $1s \rightarrow e$ transition.

The electronic structure of complexes involving the $(MoS_4)^{2-}$ and $[Ni(MoS_4)_2]^{2-}$ anions reported by Liang et al. [27] revealed that the presence of Ni in the $(MoS_4)^{2-}$ anion enhances the intensity of the valence band. This enhancement is attributed to the fact that there are more d electrons in Ni (formally d^8) than in Mo (formally d^2)

leading to observable ligand field splitting near the top of the occupied valence states.

5. Conclusions

Ni–Mo and Ni–W catalysts prepared by decomposition of impregnated thiosalts present improved catalytic activities as compared to similar catalysts prepared by coprecipitation. Intrinsic reaction rates (mol/s m^2) are more than twice higher for ITD than for HSP catalysts, similarly to other results using bis-thiometallate precursors [2]. It suggests that the ITD preparation method led to similar distribution of the precursor in the catalysts as in bis-thiometallate complexes resulting in improved catalytic activity. Structural characterization by XRD and TEM revealed that ITD catalysts show only the "poor crystalline" structure of MoS_2 (WS_2) while HSP catalysts present several phases. The improved catalytic properties are attributed to an ameliorated dispersion of the promoter in MoS_2 or WS_2 achieved through reaction (1) which is preserved during the gradual decomposition of the complex.

Acknowledgement

We are grateful to P. Bosch for help in XRD experiments, and D. Acosta and L. Rendón for HRTEM analysis.

References

[1] E.I. Stiefel, W.H. Pan, R.R. Chianelli and T.C. Ho, US Patent 4,581,125 (1986).
[2] W. Eltzner, M. Breysse, M. Lacroix and M. Vrinat, Polyhedron 5 (1986) 203.
[3] M.S. Thompson, Eur. Patent Appl. 0181035 (1986).
[4] J.A.R. van Veen, E. Gerkema, A.M. van der Kraan and A. Knoester, J. Chem. Soc. Chem. Commun. (1987) 1684.
[5] T. Shimizu, K. Hiroshima, T. Honma, T. Mochizuki and M. Yamada, Catal. Today 45 (1998) 271.
[6] S.M.A.M. Bowens, F.B.M. van Zon, M.P. van Dijk, A.M. van der Kraan, V.H.J. de Beer, J.A.R. van Veen and D.C. Koningsberger, J. Catal. 146 (1994) 375.
[7] S. Fuentes, G. Diaz, F. Pedraza, H. Rojas and N. Rosas, J. Catal. 113 (1988) 535.
[8] G. Diaz, F. Pedraza, H. Rojas, J. Cruz, M. Avalos, L. Cota and S. Fuentes, in: *Advances in Hydrotreating Catalysts*, Stud. Surf. Sci. Catal., Vol. 50, eds. M. Occelli and R.G. Anthony (Elsevier, Amsterdam, 1989) p. 91.
[9] R. Candia, B.S. Clausen and H. Topsøe, Bull. Soc. Chim. Belg. 90 (1981) 1225.
[10] D.G. Kalthod and S. Weller, J. Catal. 95 (1985) 455.
[11] R. Frety, M. Breysse, M. Lacroix and M. Vrinat, Bull. Soc. Chim. Belg. 93 (1984) 697.
[12] M. Zdrazil, Catal. Today 3 (1988) 269.
[13] M. Del Valle, M.J. Yañez, M. Avalos-Borja and S. Fuentes, in: *Hydrotreating Technology for Pollution Control*, eds. M. Occelli and R. Chianelli (Dekker, New York, 1996) p. 47.
[14] K.S. Liang, R. Chianelli, F.Z. Chien and S.C. Moss, J. Non-Cryst. Solids 79 (1986) 251.
[15] A. Mueller, E. Diemann, R. Jostes and H. Bogge, Angew. Chem. Int. Ed. Engl. 20 (1981) 934.
[16] V. Wittneben, A. Sprafke, E. Diemann and A. Muller, J. Mol. Struct. 198 (1989) 525.
[17] F. Pedraza, S. Fuentes, M. Lacroix and M. Vrinat, Catal. Lett. 62 (1999) 121.
[18] A. Vazquez, S. Fuentes and F. Pedraza, Rev. Mex. Fis. 37 (1991) 467.
[19] J.V. Sanders and K.C. Pratt, J. Catal. 67 (1981) 331.
[20] K.C. Pratt, J.V. Sanders and N. Tamp, J. Catal. 66 (1980) 82.
[21] F.B. Garreau, H. Toulhoat, S. Kasztelan and R. Paulus, Polyhedron 5 (1986) 211.
[22] L. Blanchard, J. Grimblot and J.P. Bonnelle, J. Catal. 98 (1986) 229.
[23] Y. Iwata, K. Sato, T. Yoneda, Y. Miki, Y. Sugimoto, A. Nishijima and H. Shimada, Catal. Today 45 (1998) 353.
[24] C. Gachet, M. Breysse, M. Catenot, T. Decamp, R. Frety, M. Lacroix, L. de Mourgues, J.L. Portefaix, M. Vrinat, J.C. Duchet, S. Housni, M. Lakhdar, M.J. Tilliete, J. Bachelier, D. Cornet, P. Engelhard, C. Gueguen and H. Toulhout, Catal. Today 4 (1988) 7.
[25] B.H. Cooper, A. Stanislaus and P.N. Hannerup, Hydrocarbon Process. 83 (1993).
[26] A. Mueller, W. Hellmann, J. Schneider, U. Schimanski, U. Demmer, A. Trautwein and U. Bender, Inorg. Chim. Acta 65 (1982) L41.
[27] K.S. Liang, J. Bernholc, W.H. Pan, G.J. Hughes and E.I. Stiefel, Inorg. Chem. 26 (1987) 1422.